PHYSICAL REVIEW A **78**, 051802(R) (2008)

Four-wave mixing enhanced white-light cavity

Robert Fleischhaker and Jörg Evers
Max-Planck-Institut für Kernphysik, Saupfercheckweg 1, D-69117 Heidelberg, Germany
(Received 15 June 2008; published 17 November 2008)

We discuss bandwidth enhancement of a cavity without reducing its maximum intensity buildup in a regime where the light propagation dynamics is crucial. The enhancement relies on a frequency-dependent phase compensation via negative dispersion provided by a coherently prepared atomic medium in the cavity. We analyze the spatiotemporal dynamics in such a *white-light cavity* with a full simulation of the field propagation. We find that the probe field dispersion is in addition changed by a coherent field which is generated within the medium via four-wave mixing. Counterintuitively, this in-medium dynamics leads to a further enhancement of the cavity bandwidth.

DOI: 10.1103/PhysRevA.78.051802 PACS number(s): 42.65.Sf, 42.50.Nn, 42.60.Da, 04.80.Nn

In an optical cavity, the bandwidth of supported frequencies and the intensity buildup are inversely proportional [1]. Increasing the cavity's finesse, e.g., via the reflectivity of the mirrors, leads to a higher buildup for a smaller range of frequencies and vice versa. The reason is that frequencies away from the cavity resonance correspond to different wavelengths which do not exactly fulfill the resonance condition. Thus, they acquire a phase shift with respect to the resonance frequency and experience loss at the mirrors. In terms of applications, this inverse dependence is a limiting factor for a number of schemes. Perhaps most prominently, gravitational wave detectors (GWDs) aim at detecting tiny oscillations that ideally could be amplified by the power buildup in a high-quality cavity with large bandwidth [2]. To overcome this problem, the concept of a so-called white-light cavity (WLC) was developed [3]. Its basic idea is to employ a mechanism inside the cavity that cancels the phase shift for off-resonant frequencies, thereby improving the bandwidth of a cavity without the drawback of reducing its maximum buildup. In the case of GWDs one could increase sensitivity without restricting the detection bandwidth.

It may seem that the simplest implementation of a WLC would be to insert a pair of plain parallel gratings into the cavity such that their diffraction leads to a frequency-dependent path length [4]. However, this scheme is not feasible because of the additional position-dependent phase shift caused by diffraction at a grating [5].

A different implementation of a WLC uses a medium with negative dispersion inside the cavity. In such a medium, phase shifts due to wavelength mismatch can be compensated for by suitable phase shifts generated via a frequency-dependent index of refraction. Different level schemes to achieve negative dispersion are compared in [6], and proposed WLC systems include a strongly driven double-Λ system with incoherent pumping [3], a strongly driven two-level atomic resonance, and a Λ-system off-resonantly driven by two strong fields [7]. In the latter case, the negative dispersion occurs between two gain lines. This has also been used in an experiment to demonstrate negative group velocity [8], a closely connected phenomenon, and recently the first experimental demonstration of a WLC was accomplished in such a system [9]. In a different experiment the nonlinear negative dispersion occurring in a standard Λ system at higher probe field intensities was used [10]. In this case, however, the cavity bandwidth becomes dependent on the probe field intensity. Complementary to the original WLC approach, recently a high-quality white-light cavity was demonstrated with a whispering gallery-mode resonator [11], which relies on an effectively continuous-mode spectrum, however, with rather low input and output coupling.

The experimental results show that the concept of a cavity bandwidth enhancement with a negative dispersion medium is promising. But whether a real benefit in applications beyond proof of principle will be possible with this concept will depend on the flexibility of the level scheme, scalability of its parameters, and the influence of competing or disturbing processes on the performance. Advancing to more complex level schemes than standard electromagnetically induced transparency (EIT) based setups motivated by the desire for better control over the WLC, however, typically leads to absorption in the probe or control field amplitudes throughout the propagation, severely degrading the performance in the required extended media.

In this Rapid Communication, we discuss such propagation effects in WLC media with strong control field absorption and show that, instead, the WLC bandwidth enhancement can be improved due to an electromagnetic field that is generated and sustained by the atomic medium itself via four-wave mixing (4WM). Noise amplification is avoided, as the enhancement relies on a frequency-dependent phase compensation rather than on gain. In particular, we study light propagation through an atomic four-level medium in double-Λ configuration as depicted in Fig. 1(a), which in contrast to previous WLC proposals is chosen such that propagation effects dominate the dynamics. The medium is prepared by two control fields coupling to the transitions $|1\rangle \leftrightarrow |3\rangle$ and $|2\rangle \leftrightarrow |4\rangle$, while the probe field is applied to the $|1\rangle \leftrightarrow |4\rangle$ transition. This configuration is well known to exhibit 4WM [12], resonantly enhanced to a high conversion efficiency by the double-Λ scheme. If the probe field is present, an additional field is generated within the medium on the transition $|2\rangle \leftrightarrow |3\rangle$, which in turn changes the probe field dispersion. This back-action of the probe field onto itself is a processes occurring during the propagation of the

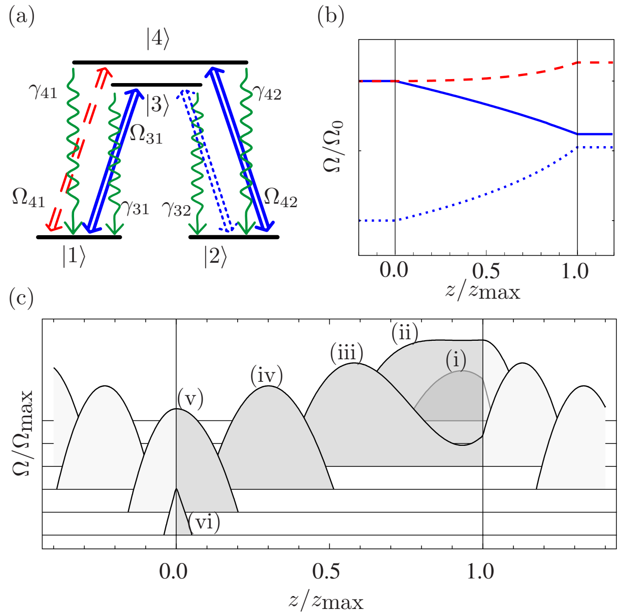

FIG. 1. (Color online) (a) The considered double-Λ level scheme. Thick solid blue lines indicate strong continuous-wave driving fields. The probe field is shown as a dashed red arrow. The dotted blue arrow represents a field generated within the medium via four-wave mixing. Ω_{jk} are Rabi frequencies. The spontaneous decays with rates γ_{jk} are denoted by the wiggly green lines ($j\in\{3,4\}$, $k\in\{1,2\}$). (b) Attenuation or amplification of the control fields (solid blue line), probe field (dashed red line), and generated field (dotted blue line) over the medium. The generated field is scaled to the initial value of the probe field. (c) Peak of a probe field pulse for successive times (i)–(vi), scaled to the respective maximum in time. The peak leaves the medium before it enters and runs through the medium in reversed direction.

light through the medium and cannot be captured in a standard treatment in terms of a single-atom susceptibility analysis. Also, the two coupling fields are absorbed such that their intensity changes substantially throughout the medium, at the same time preparing the medium in a position-dependent initial state. A typical modification of the field amplitudes in the medium is shown in Fig. 1(b). Therefore, apart from theoretical modeling, we numerically study the full propagation dynamics of all fields through the medium in order to determine their influence on the performance of a WLC.

Before we present our actual results we start by discussing an empty cavity resonance profile which is given by

$$I = I_{max}/[1+(2\mathcal{F}/\pi)^2\sin^2(\varphi/2)], \tag{1}$$

where $I_{max}=I_0/(1-r)^2$ is the maximum intensity buildup, $\mathcal{F}=\pi r^{1/2}/(1-r)$ is the cavity finesse, and $re^{i\varphi}$ is the round-trip loss and phase shift [1]. Without a medium the phase shift with respect to the resonance frequency is given by $\varphi_0=2L\Delta/c$, with L the cavity length, $\Delta=\omega-\omega_0$ the detuning from the resonance frequency ω_0, and c the speed of light in vacuum. This phase shift leads to a cavity bandwidth [full width at half maximum (FWHM)] of

$$\gamma_0 = \frac{\pi c}{L\mathcal{F}}. \tag{2}$$

A medium of length $l<L$ and refractive index n inside the cavity leads to an additional phase shift $\varphi_1=2l\omega_0(n-1)/c$. We assume that close to the resonance frequency, n can be approximated as

$$n = 1 + \frac{n_g}{\omega_0}\Delta + n_3\Delta^3 + O(\Delta^4), \tag{3}$$

where $n_g=\omega_0 \frac{\partial n}{\partial\omega}|_{\omega_0}$ is the group index and $n_3=\frac{1}{6}\frac{\partial^3 n}{\partial\omega^3}|_{\omega_0}$ is the third-order correction term to a linear slope. The second-order term vanishes since in our system the resonance frequency is an inflection point of the dispersion if probe field frequency and cavity resonance coincide. From the WLC condition $\varphi_0+\varphi_1=0$ we find

$$n_g = -L/l. \tag{4}$$

Now the terms linear in frequency cancel and the enhanced cavity bandwidth is given by (FWHM)

$$\gamma_1 = \left(\frac{4\pi c}{l\omega_0 n_3 \mathcal{F}}\right)^{1/3}. \tag{5}$$

From the WLC condition [Eq. (4)] we see that a WLC requires a medium with negative group velocity. Therefore, in a first calculation, we propagate probe pulses of different bandwidths through the double-Λ medium and optimize parameters for a negative group index. For this, we derive the Maxwell-Schrödinger equations describing the light propagation through the medium using standard techniques [16] and solve the equations numerically on a grid using a Lax-Wendroff integration method [17]. We assume a $l=0.3$ m long medium with a density of $N=6.6\times10^{15}\text{m}^{-3}$ of sodium atoms and initial control field strengths of $\Omega_{42}=15.5\gamma$ and $\Omega_{31}=16\gamma$. The weak probe field ($\Omega_{41}=0.1\gamma$) is applied to the transition $|1\rangle\leftrightarrow|4\rangle$. For a Gaussian probe field envelope the peak of the pulse leaves the medium before it enters and runs through the medium in a reversed direction [see Fig. 1(c)]. This behavior is typical for a medium with negative group velocity [8,18]. From the advancement in time T_a of the pulse peak after passing the medium, we calculate the group index $n_g=-cT_a/l$.

As we are most interested in propagation effects, the evolution of the different field amplitudes throughout the medium is shown in Fig. 1(b). The control fields are attenuated to about 60% of their initial value. At the same time, the control fields together with the probe field generate an additional field on the transition $|2\rangle\leftrightarrow|3\rangle$ via 4WM. This internally generated field and the externally applied fields form a closed interaction loop [13–15], which in turn leads to light scattering into the probe field mode. By means of this backaction, the probe field dispersion is changed as we will see later. Furthermore, the probe field is amplified by about 10%, which allows one to compensate for losses inevitable in an experimental realization.

To evaluate the medium performance, in a second calculation, we extract the effective medium susceptibility by comparing amplitude and phase of a continuous-wave probe field at the medium entry and exit after full numerical propa-

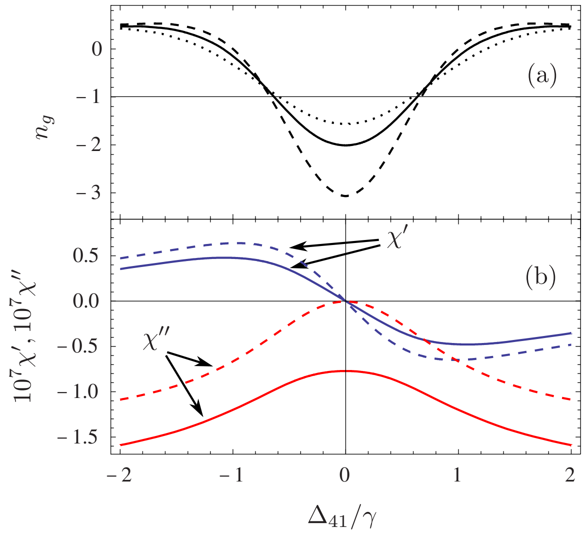

FIG. 2. (Color online) (a) Group index of a Gaussian probe pulse with bandwidth of 2γ (dotted line) and $\gamma/2$ (solid line). The dashed line shows the bandwidth $\gamma/2$, but with field generation via 4WM suppressed. Bandwidth narrowing below $\gamma/2$ does not change the group index significantly. (b) Real part χ' (upper blue lines) and imaginary part χ'' (lower red lines) of the effective probe field susceptibility with (solid lines) and without (dashed lines) 4WM.

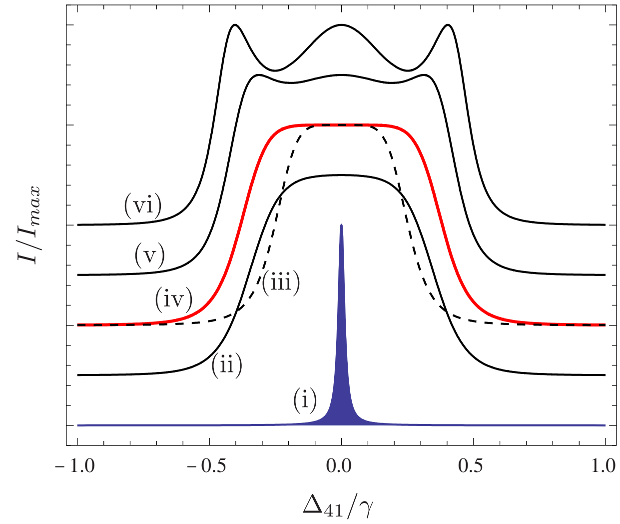

FIG. 3. (Color online) Intensity buildup for an $\mathcal{F}=1000$ cavity without medium (i) and with the proposed WLC medium (iv). Curve (iii) shows the corresponding medium result with four-wave mixing artificially suppressed. The other three profiles show the general case with 4WM and a 2% (ii), a −2% (v), and a −4% (vi) mismatch of the cavity length with respect to the WLC condition. For better visibility the different profiles have been shifted by multiples of 0.25 with respect to each other. Profiles (iii) and (iv) have the same shift.

gation, simulating an experimental measurement. For this, we relate the probe field at the medium exit, $\Omega_{41}(l)$, to the initial field $\Omega_{41}(0)$ by

$$\Omega_{41}(l) = \Omega_{41}(0)e^{-kl\chi''/2}e^{ikl\chi'/2}, \tag{6}$$

where k is the respective wave number, whereas χ' and χ'' are the real and imaginary parts of the effective susceptibility. The obtained susceptibility describes a single pass of the probe field through the medium.

The results for the group index and the effective susceptibility are shown in Fig. 2 against the probe field detuning. In addition, we also show as dashed lines the corresponding susceptibility that is obtained if the medium back-action via 4WM and the closed-loop scattering are suppressed. This is achieved by artificially setting the generated field on the transition $|2\rangle \leftrightarrow |3\rangle$ to zero throughout the numerical analysis. In the latter case, the effective susceptibility can be perfectly explained by averaging the result of a single-atom analysis over the nonuniform control field intensities in the medium. In contrast, in the general case with 4WM and medium back-action present, a single-atom analysis combined with an averaging fails to give the correct results.

It can be seen from Fig. 2 that the probe field dispersion with 4WM has both smaller slope and group index than without a back-action [Figs. 2(a) and 2(b), solid lines]. It may seem that a smaller group index deteriorates the bandwidth enhancement. But as long as the group index for a resonant pulse reaches values below $n_g=-1$, the WLC condition, Eq. (4), can be fulfilled if the ratio of medium length to cavity length is suitably adjusted. In our numerical calculation, we find $n_g \simeq -2$, which corresponds to a medium filling about half of the cavity.

In Fig. 3, we finally show the enhanced cavity resonance profile. We assume a cavity finesse of $\mathcal{F}=1000$, which corresponds to a mirror reflectivity of $r=99.68\%$, and a cavity length of $L=59.5$ cm for which the WLC condition is fulfilled in the case with 4WM. With 4WM suppressed, the negative group index is larger such that the WLC condition is violated for the same parameters. We compensate for this by adjusting the medium length l suitably, but keep the cavity length L fixed such that the empty cavity bandwidth γ_0 remains equal. Without 4WM, the cavity bandwidth is enhanced by about a factor of 20 [Fig. 3(iii)]. With 4WM, the enhancement is by a factor of about 30 [Fig. 3(iv)]. Thus, the in-medium dynamics enhances the desired bandwidth increase.

At the WLC condition, the enhanced bandwidth profiles become quadratically flat around the resonance frequency. Under- or overcompensating for the frequency-dependent phase shift leads to a less flat response; see Fig. 3. Similarly, the bandwidth enhancement depends on the control field intensity and thus on the transverse distance x to the control field center axis. We assumed a Gaussian control field intensity profile with width σ_c and show the spatial enhancement variation in Fig. 4(a). For comparison, intensity profiles of probe beams with widths $\sigma_c/3$ and $\sigma_c/10$ are shown as shaded areas. Full bandwidth enhancement is achieved up to about $x=0.25\sigma_c$.

We also calculated the cavity bandwidth enhancement for different values of empty cavity bandwidth and for both cases, with and without 4WM. The result is shown in Fig. 4(b) in a double-logarithmic plot. Both curves are indistinguishable from the theoretical power law $\gamma_1/\gamma_0 \propto (\gamma_0/\gamma)^{-2/3}$, which is evident from Eqs. (2) and (5).

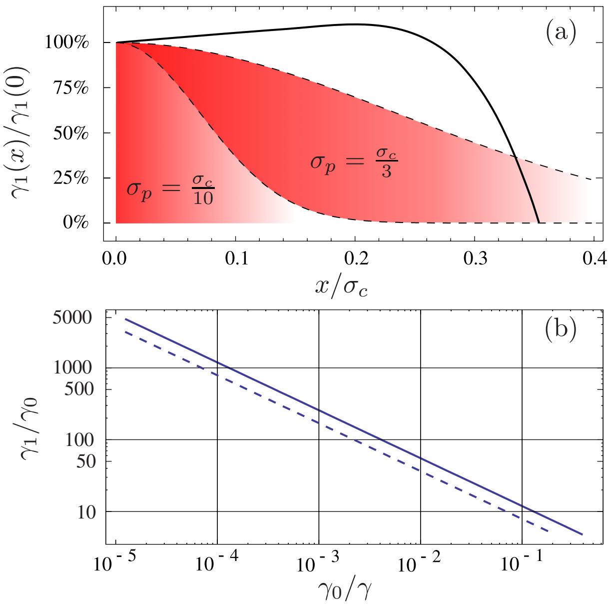

FIG. 4. (Color online) (a) Cavity bandwidth throughout a Gaussian transverse control field intensity profile with width σ_c (solid line). Shaded areas indicate probe beam intensity profiles with widths $\sigma_c/3$ and $\sigma_c/10$. (b) Enhancement factor with (solid line) and without (dashed line) the in-medium generated 4WM field against empty cavity bandwidth γ_0.

From Fig. 4(b), bandwidth enhancement factors above 10^3 are theoretically predicted for high-quality cavities. This result, however, neglects practical issues common to light propagation setups with gases as follows. In an atomic gas medium suitable for the required phase compensation, typically Doppler effects need to be considered. In existing experiments (see, e.g., [8–10]), this issue could be overcome. As far as the propagation effects in our level scheme are concerned, the relevant processes are two-photon Raman transitions and four-photon closed-loop transitions. For these transitions the Doppler effect typically cancels to first order at the resonance frequency if the fields copropagate. However, since the mechanism for a WLC relies on a frequency range around the resonance frequency, quantitative changes to our results can be expected. Second, an exact fulfilling of the WLC condition requires a stabilization of the different parameters such as the control field strengths and the cavity length. From Figs. 3(ii), 3(v), and 3(vi) and Fig. 4(a), it can be seen that a WLC condition mismatch on the few percent level typically is not critical. As far as the application of a WLC in a GWD is concerned, in principle the bandwidth enhancement factor should be directly convertible into a sensitivity enhancement of the same order. A question that has to be addressed, however, is how to actually implement a WLC into a GWD. Especially the larger scales of the cavity in the case of existing GWDs [2] consisting of the interferometer and a so-called signal recycling mirror pose a demanding task.

In summary, we have investigated a white light cavity enhanced by in-medium propagation dynamics. The probe field generates an additional light field via four-wave mixing during the light propagation. The presence of the additional field in turn changes the probe field dispersion which leads to a further bandwidth enhancement.

J.E. would like to thank M. S. Zubairy for helpful discussions.

[1] B. E. A. Saleh and M. C. Teich, *Fundamentals of Photonics* (Wiley, New York, 1991).
[2] P. Aufmuth and K. Danzmann, New J. Phys. **7**, 202 (2005).
[3] A. Wicht *et al.*, Opt. Commun. **134**, 431 (1997).
[4] S. Wise *et al.*, Class. Quantum Grav. **21**, S1031 (2004).
[5] S. Wise *et al.*, Phys. Rev. Lett. **95**, 013901 (2005).
[6] A. Wicht, R. H. Rinkleff, L. S. Molella, and K. Danzmann, Phys. Rev. A **66**, 063815 (2002).
[7] R. H. Rinkleff and A. Wicht, Phys. Scr., T **T118**, 85 (2005).
[8] A. Dogariu, A. Kuzmich, and L. J. Wang, Phys. Rev. A **63**, 053806 (2001).
[9] G. S. Pati, M. Salit, K. Salit, and M. S. Shahriar, Phys. Rev. Lett. **99**, 133601 (2007).
[10] H. Wu and M. Xiao, Phys. Rev. A **77**, 031801(R) (2008).
[11] A. A. Savchenkov, A. B. Matsko, and L. Maleki, Opt. Lett. **31**, 92 (2006).
[12] Maneesh Jain, H. Xia, G. Y. Yin, A. J. Merriam, and S. E. Harris, Phys. Rev. Lett. **77**, 4326 (1996); S. Babin *et al.*, Opt. Lett. **21**, 1186 (1996); B. Lü, W. H. Burkett, and M. Xiao, *ibid.* **23**, 804 (1998); D. A. Braje, V. Balic, S. Goda, G. Y. Yin, and S. E. Harris, Phys. Rev. Lett. **93**, 183601 (2004).
[13] S. J. Buckle *et al.*, Opt. Acta **33**, 1129 (1986).
[14] M. Mahmoudi and J. Evers, Phys. Rev. A **74**, 063827 (2006).
[15] R. Fleischhaker and J. Evers, Phys. Rev. A **77**, 043805 (2008).
[16] M. O. Scully and M. S. Zubairy, *Quantum Optics* (Cambridge University Press, Cambridge, England, 1997).
[17] W. H. Press, B. P. Flannery, S. A. Teukolsky, and W. T. Vetterling, *Numerical Recipes* (Cambridge University Press, Cambridge, England, 1992).
[18] P. W. Milonni, *Fast Light, Slow Light and Left-Handed Light* (Institute of Physics, Bristol, 2005).